JOURNAL OF SPACECRAFT AND ROCKETS
Vol. 32, No. 5, September–October 1995

Dissociative Cooling: Effect on Stagnation Heat Transfer of Gas Mixture Injection

Benjamin P. Lacy,* Dennis E. Wilson,† and Philip L. Varghese‡
University of Texas at Austin, Austin, Texas 78712

By embedding a dissociating material into the porous outer structure of a projectile, stagnation-point heat transfer may be reduced by transpiration cooling resulting from the outflow of the dissociated gas products. The principal material considered is ammonium chloride, NH_4Cl, which dissociates at temperatures over 613 K, hence providing additional heat-transfer reduction. Stagnation-point heat-transfer solutions for the injection of the dissociation products of NH_4Cl into both equilibrium and frozen boundary layers are presented and compared with those for the injection of other gases such as helium. Results show that dissociative cooling has the potential to provide a significant reduction in stagnation-point heat transfer as temperatures rise, because the gas injection rate increases with the temperature of the NH_4Cl interface.

Nomenclature

C = $\rho\mu/(\rho\mu)_e$
c_i = mass fraction, ρ_i/ρ
c_p = specific heat per unit mass at constant pressure
$\bar{c}_p$ = mass-average specific heat of gas mixture
D = multicomponent diffusion coefficient
$\mathcal{D}$ = binary-diffusion coefficient
f = quantity defined by Eq. (8)
h = enthalpy
j = diffusive mass flux
k = thermal conductivity
ℓ = $\rho\mu/(\rho\mu)_w$
Le = Lewis number, $D_\rho \bar{c}_p/k$
M = molar mass
$\dot{M}$ = blowing parameter, $\rho_w v_w/\sqrt{\rho_e \mu_e \kappa}$
$\dot{N}$ = molar flux
Nu = Nusselt number, $q_w'' x/(T_e - T_w)k$
P = pressure
Pr = Prandtl number, $\mu\bar{c}_p/\kappa$
q'' = heat flux
R = gas constant
r = cylindrical radius
Re = Reynolds number, $u_e x/\nu$
T = temperature
u = x-component velocity
v = y-component velocity
x = distance along body surface
y = distance normal to body surface
ε = well depth in intermolecular potential
η = transformation defined by Eq. (6)
θ = T/T_e
κ = velocity gradient, $\partial u_e/\partial x$
μ = viscosity
ν = kinematic viscosity
ξ = transformation defined by Eq. (7)
ρ = density
σ = collision diameter
Φ_{ij} = function of molar masses, $\sqrt{M_j/M_i}$
ϕ = porosity
χ_i = mole fraction of species i
Ω_D = diffusion collision integral
ω_i = mass rate of species formation

Subscripts and Superscripts

e = boundary-layer edge
f = formation
i = ith species
int = interface of dissociating material
j = index that defines flow as two dimensional or axisymmetric
m = mixture
n = total number of species
tr = monatomic value of thermal conductivity
w = wall

Introduction

THE use of transpiration cooling to reduce stagnation-point heat transfer has been demonstrated to have significant potential in a number of analytical and experimental investigations.[1–10] One variation on transpiration cooling was presented by Camberos and Roberts.[11] They suggested use of an internal ablator placed behind a porous outer nose. Vaporized gas from the ablator would flow out through the porous outer surface, providing transpiration cooling. The present report investigates a further variation on transpiration cooling called dissociative cooling.

Dissociative cooling involves the embedding of a dissociating material into the porous outer structure of a projectile (Fig. 1). The principal material considered here is ammonium chloride, NH_4Cl. Ammonium chloride begins to dissociate[12] into ammonia and hydrogen chloride at temperatures over 613 K. As the resulting gases flow through the porous structure to the hotter outer surface, the gas temperature will increase further and the ammonia will begin to break down into nitrogen and hydrogen. These dissociations will

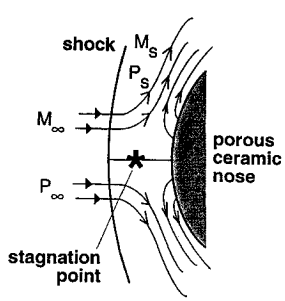

Fig. 1 Dissociative cooling concept.

Received Feb. 15, 1994; revision received Dec. 2, 1994; accepted for publication Dec. 2, 1994.

*Graduate Research Assistant, Institute for Advanced Technology, 4030-2 W. Braker Lane. Student Member AIAA.
†Associate Professor, Institute for Advanced Technology, 4030-2 W. Braker Lane. Member AIAA.
‡Professor, Aerospace Engineering. Senior Member AIAA.

absorb energy that would have otherwise gone to heating the projectile. The out flowing gas mixture will provide transpiration cooling, which reduces the heat transfer to the surface.

Ammonium chloride has been chosen for study because of its material properties. It has a high enthalpy of dissociation, around 3100 kJ/kg. Other materials such as aluminum nitride and boron nitride have even greater enthalpies of dissociation but dissociate at much higher temperatures. The dissociation temperature of ammonium chloride is low enough to provide thermal protection when needed, but not so low that all of the ammonium chloride will have dissociated before the projectile's flight is completed.

Previous work[1,2] examined the effect of air-to-air injection. Weston[9] examined the case of equilibrium dissociating air injection. Several reports[3–6] have looked at the effects of the injection of helium. Sparrow et al.[4] examined the effect on heat transfer and recovery temperature of the Dufour effect (concentration-gradient-driven heat transfer) for a number of different single-species gases. This paper showed that the Dufour effect is most significant for the injection of low-molecular-weight gases at high injection rates with wall temperatures close to the boundary-layer edge temperature. Sparrow et al.[6] also examined the effects of both thermal diffusion (heat-transfer-driven diffusive flux) and the Dufour effect on heat transfer for helium injection at the stagnation point. This report showed that the Dufour effect had a much greater effect on heat transfer than did thermal diffusion. Henline[10] used the BLIMPK code to compare heat-transfer rates for the injection of different single-species gases under single-stage-to-orbit conditions, with finite-rate surface reactions. All of these papers showed that transpiration flow could reduce the convective heating to the stagnation point, with low-molecular-weight gases being most effective, particularly at high flow rates.

However, little work has been done on injection of multiple-species gas mixtures. Solutions for the injection of a gas mixture at the stagnation point are needed in order to examine the potential of dissociative cooling more thoroughly. These solutions examine the limiting cases of both a frozen and an equilibrium boundary layer.

Mathematical Model

The compressible boundary-layer equations to be solved are as follows[13,14]:

1) Continuity equation:

$$\frac{\partial(\rho u r^j)}{\partial x} + \frac{\partial(\rho v r^j)}{\partial y} = 0 \tag{1}$$

where $j = 0$ for two-dimensional flow, $j = 1$ for axisymmetric flow.

2) Species continuity equation:

$$\rho u \frac{\partial c_i}{\partial x} + \rho v \frac{\partial c_i}{\partial y} = -\frac{\partial}{\partial y}\left(\rho \sum_{j \neq i} \frac{M_i M_j}{M^2} D_{ij} \frac{\partial \chi_j}{\partial y}\right) + \omega_i \tag{2}$$

3) Momentum equations:

$$\rho u \frac{\partial u}{\partial x} + \rho v \frac{\partial u}{\partial y} = \frac{\partial}{\partial y}\left(\mu \frac{\partial u}{\partial y}\right) - \frac{\partial P}{\partial x} \tag{3}$$

$$\frac{\partial P}{\partial y} = 0 \tag{4}$$

4) Energy equation:

$$\rho u \bar{c}_p \frac{\partial T}{\partial x} + \rho v \bar{c}_p \frac{\partial T}{\partial y} = \frac{\partial}{\partial y}\left(k \frac{\partial T}{\partial y}\right) + \mu\left(\frac{\partial u}{\partial y}\right)^2 + u \frac{\partial P}{\partial x}$$

$$- \sum_i c_{pi} \rho \sum_{j \neq i} \frac{M_i M_j}{M^2} D_{ij} \frac{\partial \chi_j}{\partial y} \frac{\partial T}{\partial y} - \sum_i \omega_i h_i \tag{5}$$

In these equations both thermal diffusion and the Dufour effect have been ignored. In view of the conversion of ammonia to hydrogen to water, this paper examines several limiting cases: a frozen boundary layer with frozen injectants for both a fully catalytic and noncatalytic wall, and an equilibrium boundary layer with both frozen and equilibrium injectants. For the equilibrium boundary-layer case additional equations relating the equilibrium concentrations of the gases are needed and provide elemental conservation for the species continuity equation. For air the reactions are taken as $O_2 \leftrightarrow 2O$ and $N_2 + O_2 \leftrightarrow 2NO$. For the ammonia injectant three separate cases are considered: frozen NH_3; equilibrium $NH_3 \leftrightarrow 0.5N_2 + 1.5H_2$, where the hydrogen does not react to form H_2O; and $2NH_3 + 1.5O_2 \leftrightarrow N_2 + 3H_2O$, where the ammonia is assumed to react completely to form water. The speed of reaction of the hydrogen with oxygen in the boundary layer will determine which model is most suitable. At the temperatures involved it is reasonable to assume HCl is nonreacting.

The flow equations are transformed to ordinary differential equations using the similarity transformations[15]

$$\eta = \frac{r u_e}{\sqrt{2\xi}} \int_0^y \rho \, dy \tag{6}$$

$$\xi = \int_0^x \rho_w \mu_w u_e r^2 \, dx \tag{7}$$

and the dimensionless dependent variables

$$f' = (u/u_e) \tag{8}$$

$$\theta = T/T_e \tag{9}$$

Transforming the equations of flow and eliminating the ξ dependence at the stagnation point gives the following[14,16]:

$$-\left(\frac{\ell}{Pr} \sum_{j \neq i} \frac{M_i M_j}{M^2} Le_{ij} \chi_j'\right)' + f c_i' + \frac{\beta}{\kappa} \frac{\omega}{\rho} = 0 \tag{10}$$

$$(\ell f'')' + f f'' + \frac{1}{2}\left(\frac{\rho_e}{\rho} - (f')^2\right) = 0 \tag{11}$$

$$\left(\frac{\bar{c}_p \ell}{Pr} \theta'\right)' + \bar{c}_p f \theta' - \sum_i \frac{c_{pi} \ell}{Pr} \sum_{j \neq i} \frac{M_i M_j}{M^2} Le_{ij} \chi_j' \theta'$$

$$- \frac{\beta}{\kappa} \frac{\sum_i \omega_i h_i}{\rho T_e} = 0 \tag{12}$$

where $\bar{c}_p = \sum_i c_i c_{pi}$ and $\rho_e/\rho = \theta(\sum_i c_i R_i)/R_e$.

The boundary conditions are $f'(0) = 0$, $f'(\infty) = 1$, $\theta(0) = \theta_w$, $\theta(\infty) = 1$, $c_{\text{air}}(\infty) = 1$, and $f_w = -v_w/\sqrt{2\nu_w \kappa}$. The last boundary condition is derived from the continuity equation, assuming the injection rate is a known quantity. The edge concentrations of all the foreign injectants are zero; the edge concentrations of the products of air are determined from the equilibrium relations at the boundary-layer edge temperature and pressure. The wall concentrations are the remaining boundary conditions to be defined. For the equilibrium case the wall temperature will be assumed low enough so that the concentrations of O and NO will be zero at the wall, as they are for the frozen boundary layer and catalytic wall. The concentration of the remaining species (and O and NO for the frozen boundary layer and noncatalytic wall) are determined from a flux balance of species at the wall. The mass balance will consist of any blowing of species from the wall, any diffusion of species at the wall, any creation at the wall (as of O_2 and N_2 for the frozen boundary layer with catalytic wall), and any influx (as in the case where H_2O flows from the interior and O_2 flows into the interior). The blowing from the wall of a species is determined by the specified injection rate and the fact that equal amounts of NH_3 and HCl are produced by dissociation of NH_4Cl. In the equilibrium case a certain amount of the injected flow will exit the surface as N_2 and H_2, or N_2 and H_2O. In the case where H_2O forms, at higher blowing rates the rate of H_2 flowing from the wall will be greater than the flux of O_2 to the wall. At equilibrium all the NH_3 and H_2 will react

to form water as long as sufficient O_2 is available. Hence, at higher blowing rates the formation of H_2O is assumed to occur within the boundary layer at a flame sheet,[17] where the flux of hydrogen atoms equals twice the flux of oxygen atoms. Additionally, θ at the flame sheet has to be such that the heat transfer from that point matches the enthalpy of formation of the water reaction.

The species injection is related to wall concentrations by balancing the species flowrates at the wall with the known overall injection rate and the known rate at which each element is injected. This can be done using the equation for the diffusive flux:

$$j_{iw} = \rho_{iw}(v_{iw} - v_w) \tag{13}$$

$$j_{iw} = \frac{\rho_w^2}{M_w^2} \sum_{j \neq i} M_i M_j D_{ij} \chi_j' \left(\frac{2\kappa}{\rho_w \mu_w} \right)^{\frac{1}{2}} \tag{14}$$

The relation to wall mole fraction becomes

$$\chi_i = \frac{\rho_w}{M_i M_w (v_{iw} - v_w)} \sum_{j \neq i} M_i M_j D_{ij} \chi_j' \left(\frac{2\kappa}{\rho_w \mu_w} \right)^{\frac{1}{2}} \tag{15}$$

For the mass flux of a given species, the wall concentration can be related to the concentration gradients, so that wall concentration may be solved for iteratively.

Heat-Transfer Rates

Once a solution has been obtained, heat-transfer rates can be determined. At the stagnation point, neglecting the Dufour effect, the surface heat transfer is defined here as the conduction term plus the energy release at the wall due to any catalytic reaction at the wall of N and O:

$$q_w'' = k_w \frac{\partial T}{\partial y_w} - \sum (\rho v)_{iw} h_{if} \tag{16}$$

Using Eqs. (8) and (9), Eq. (16) can be transformed into

$$q_w'' = k_w \theta_w' T_e \sqrt{2\kappa / v_w} - \sum (\rho v)_{iw} h_{if} \tag{17}$$

Expressing this nondimensionally, we have

$$\frac{Nu}{\sqrt{Re_e}} = \frac{q_w'' \sqrt{v_e/\kappa}}{(T_e - T_w) k_e} \tag{18}$$

This paper does not examine possible radiation effects. Howe[18] showed that for a transpiring gas to have a significant effect in shielding a body from incident radiation from the shock layer at the stagnation point, the injected gas would have to have an extremely high absorption coefficient. It follows that the same would be true for emission of radiation by the transpiring gas, since for most cases (except for the flame wall) the boundary layer will be cooler than the shock layer, and in all cases thinner. Dissociative cooling should therefore have little effect on the intensity of radiation striking the body.

The flow of the H_2 and NH_3 downstream of the stagnation point could have a negative (or positive) effect on heat transfer away from the stagnation point due to possible chemical reactions by these species. However, the growth of the boundary layer and the drop in concentration of these gases away from the stagnation point should make the results of any chemical reactions negligible compared to the rapid drop in heat transfer away from the stagnation point.

Another possible effect is of transpiration promoting an early transition to turbulence and thereby increasing heat transfer to the body. Transition is also influenced by the wall temperature ratio θ_w and the streamwise pressure gradient. E. R. van Driest[19] showed that cooling the surface can stabilize the boundary layer. Concurrently, an adverse pressure gradient, such as that caused by the shape change of a body undergoing ablation, can induce transition. So, though it is possible that surface blowing can produce premature transition, it is also possible that a properly designed system can have a more stable boundary layer than an unprotected body, due to the reduction in body surface temperature and maintaining a favorable dp/dx.

Solution Procedure

The similarity equations with appropriate boundary conditions are solved on a SPARCstation IPC. The equations are solved using repeated shooting runs (with Newton iteration), until the wall concentrations meet the appropriate boundary conditions, using at least 500 points to ensure grid convergence. For the frozen boundary layer the solution involves making an initial guess of the wall concentration of the components of air (including NO and O for a noncatalytic wall) and $j - 1$ of the j injected gases for the selected injection rate. An initial guess of wall gradients is also made. The shooting procedure repeatedly marches through space, solving the equations and then modifying the wall gradients until the solution matches the declared boundary-layer edge conditions.

The new wall concentration gradients can then be used to solve for new wall concentrations from the wall boundary-condition relations. Since the solution will not necessarily converge using the new wall concentrations, new guesses are made, and the whole process is repeated until the concentrations found from the boundary conditions match the guesses exactly. During this whole process, property relations are constantly updated according to the new wall concentrations.

For the equilibrium boundary layer the concentrations of N_2, O_2, and H_2 (NH_3) are guessed through the entire boundary layer. The concentrations of the products of these gases can then be determined through the equilibrium relations for the reactions defined earlier. Using the species continuity equation for each of these products, the species production terms can be determined at each point in the boundary layer using finite-difference techniques. The concentration gradients of these product gases through the boundary layer are also found in this manner and can then be used to find the wall fluxes of the various species using the diffusive flux relations given earlier. Then, as with the frozen boundary layer, the shooting procedure can be used to solve the equations through the boundary layer. The newly determined concentrations of N_2, O_2, and H_2 can now be used to again determine the concentration of product gases. As before, new wall concentrations are selected, and the whole process is repeated until all boundary conditions are met.

For the case of H_2O formation, the similarity equations must be solved from the wall to the flame sheet, and from the flame sheet to the boundary-layer edge once H_2O formation moves into the boundary layer. The location of the flame sheet is the point where the flux of hydrogen atoms equals twice the flux of oxygen atoms. The concentrations of H_2, O_2, NO, and O are zero at this point. The concentration of the other species at the flame sheet must be such that the species fluxes along with the species creation will match across it. The temperature ratio at the flame sheet is set so that heat transfer from the flame sheet matches the enthalpy of formation of water reaction.

Once all boundary conditions have been met, the temperature gradients (along with any fluxes of NO and O at the wall) can be used to determine the heat transfer to the surface. Solutions given here are in terms of the blowing parameter

$$\dot{M} = \frac{\rho_w v_w}{\sqrt{\rho_e \mu_e \kappa}} \tag{19}$$

This parameter was selected instead of f_w to be consistent with the presentation method used by Sparrow et al.[4] We present here results in terms of $Nu/\sqrt{Re_e}$.

Ammonium Chloride Injection Rate

To evaluate the effectiveness of the ammonium chloride dissociation in providing transpiration cooling, a dissociation rate as a function of temperature is required. Virnich and Höpfner[20] provide the forward reaction rate as a function of temperature at low temperatures based on experiment. By extrapolating and fitting with a $\ln\dot{N}$-vs-$1/T$ relationship, the following relationship is obtained (see Fig. 2):

$$\dot{N} = 9689 e^{-6126.4/T_{\text{int}}} \phi \text{ mol/s m}^2 \tag{20}$$

or, in terms of the blowing parameter,

$$\dot{M} = \frac{517.9 e^{-6126.4/T_{\text{int}}} \phi}{\sqrt{\rho_e \mu_e \kappa}} \text{ kg/s m}^2 \tag{21}$$

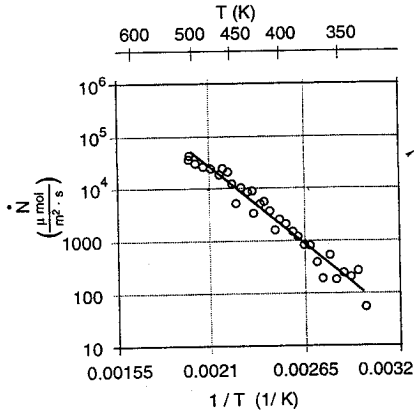

Fig. 2 NH_4Cl dissociation rate.

Since the products of dissociation are flowing to a region of higher temperature, the forward reaction rate is taken as the actual dissociation rate, which equals the injection rate. With a given ammonium chloride interface temperature, the injection rate can then be determined and the reduction in heat transfer due to the dissociation of ammonium chloride can be seen for the given flow conditions.

Results

As a check, runs for air-to-air injection were made for $C = 1$ through the boundary layer, and the results were found to match those of Ref. 1. With variable thermal properties, the results for helium agree well with Ref. 5. In all runs the boundary-layer edge was assumed to be in equilibrium. The edge concentrations of the products of air are determined from the equilibrium relations at the boundary-layer edge temperature and pressure. The temperature and pressure behind the shock is found from the compressible flow equations and the Mollier tables for equilibrium air based on the desired flight conditions. The edge temperature and pressure can be determined from the gas velocity going to zero at the stagnation-point boundary-layer edge and using the Newtonian pressure relation.

Figure 3 shows heat transfer vs $\dot{M}$ for different gases, including the frozen products of ammonium chloride (NH_3 and HCl), injected into an equilibrium air boundary layer for an axisymmetric blunt-body projectile traveling at sea level at Mach 8 and $\theta_w = 0.25$, and $T_w = 786$ K. The blowing uniformly reduces the temperature gradient and hence the heat transfer. As can be seen, the NH_3–HCl mixture is superior to air at all injection rates and superior to helium at low injection rates. This is due to helium's high thermal conductivity outweighing the effect of the high specific heat for low injection rates. Otherwise, the results follow the general rule that the lower the molecular weight of a gas, the more effective it is as a coolant.

Figure 4 shows heat transfer for the same flight conditions but with the ammonium chloride products in equilibrium. For the case without water formation, at low injection rates, NH_3 flows out and breaks down into H_2 and N_2, some of which flows back into the wall. At higher flow rates both NH_3 and H_2 flow from the wall. At all injection rates the wall concentrations of H_2 are much higher than for NH_3. The breakdown of the remaining NH_3 in the boundary layer causes some reduction in heat transfer. For the case with H_2O formation, all of the NH_3 converts to H_2O in the interior until the flux of O_2 is no longer sufficient to match the H_2O flow out. Until this point, the heat transfer is about the same as for the frozen-NH_3 case. Once injection becomes great enough, H_2O formation moves out into the boundary layer, and heat transfer to the wall undergoes a large jump. As blowing further increases, heat transfer drops as the flame sheet is pushed out further into the boundary layer. Figure 5 shows the concentration of O_2, N_2, H_2, and H_2O and the temperature ratio through the boundary layer for such a case, $\dot{M} = 1.0$, where the flame sheet is at $\eta = 1.46$ (approximately 50% of the boundary-layer thickness). N_2 has a small peak at the flame sheet from the breakdown of NO, which also contributes to the heat-transfer increase. It should be noted that for all cases where reactions occur in the interior (NH_3 dissociation, H_2O formation), the effectiveness of the process depends on the effect

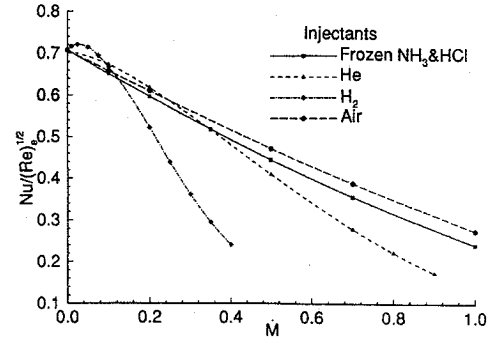

Fig. 3 Heat-transfer parameter vs injection rate in equilibrium air boundary layer.

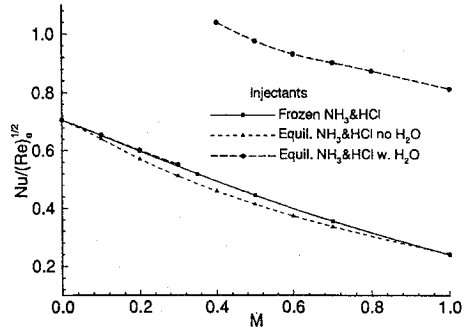

Fig. 4 Heat-transfer reduction for nonreacting NH_3 vs NH_3 in equilibrium.

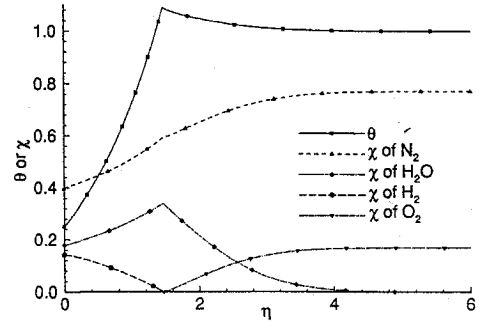

Fig. 5 Effect of H_2O formation on boundary-layer temperatures and concentrations.

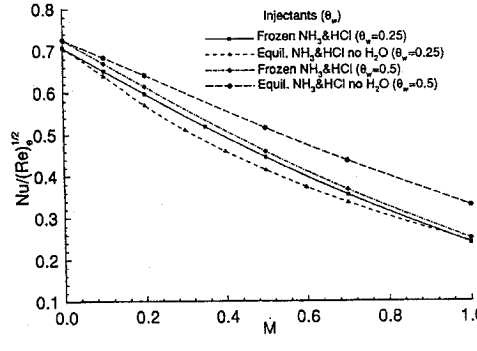

Fig. 6 Effect of ratio of surface to bulk temperature on heat-transfer parameter vs injection rate.

these reactions have on the heating rate of the projectile. As can be seen from the heat-transfer jump in the case with H_2O, this can be significant.

Figure 6 shows the effect on the heat-transfer parameter of wall temperature variation. The effect is only large for the case of reacting NH_3, since at higher wall temperatures the injectant is mostly N_2 and HCl (with the much smaller injection mass of H_2), and with few reactions occurring in the boundary layer.

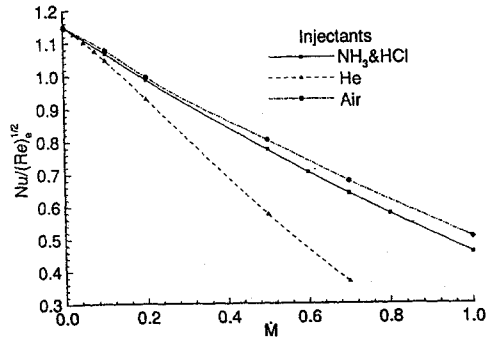

Fig. 7 Heat-transfer parameter vs injection rate for a frozen boundary layer with a catalytic wall.

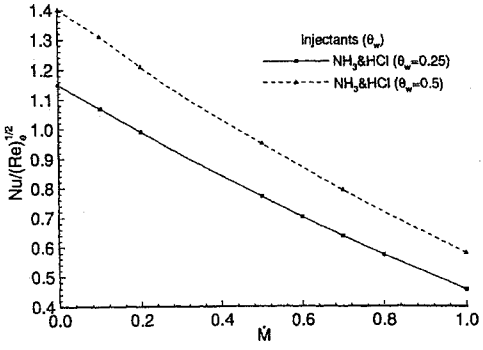

Fig. 8 Effect of ratio of surface to bulk temperature on wall heat-transfer parameter vs injection rate for a frozen boundary layer with a catalytic wall.

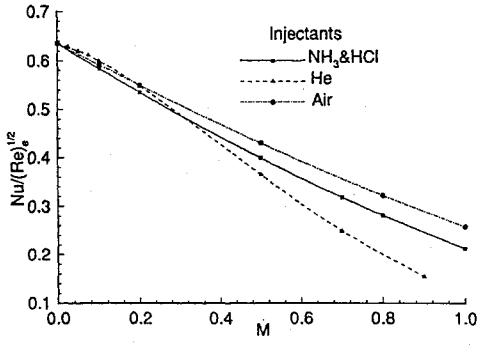

Fig. 9 Heat-transfer parameter vs injection rate for a frozen boundary layer with a noncatalytic wall.

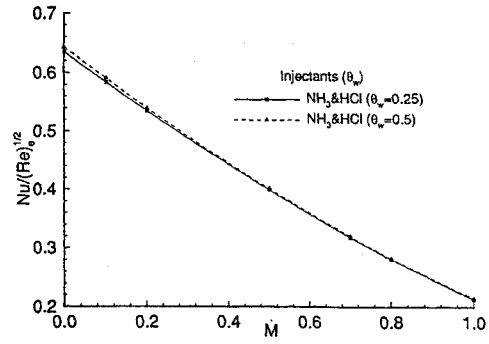

Fig. 10 Effect of ratio of surface to bulk temperature on wall heat-transfer vs injection rate for a frozen boundary layer with a noncatalytic wall.

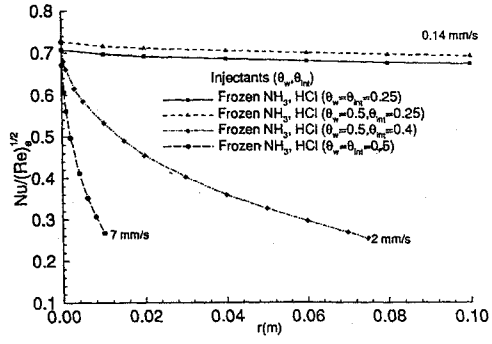

Fig. 11 Effect of NH_4Cl interface temperature on heat-transfer parameter as a function of blunt-body radius for a equilibrium air boundary layer.

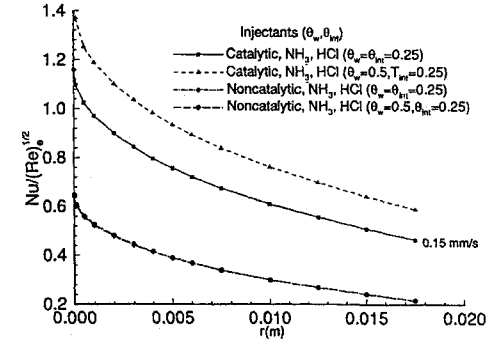

Fig. 12 Effect of NH_4Cl interface temperature on heat-transfer parameter as a function of blunt-body radius for a frozen boundary layer.

Figure 7 shows heat transfer for the frozen-boundary-layer case with fully catalytic wall (again $\theta_w = 0.25$) and frozen injectants. The boundary-layer edge conditions are calculated for a blunt-body projectile traveling at 54.9 km (180,000 ft) at Mach 10. The recombination of air products at the wall makes heat transfer uniformly higher. Again the ammonium chloride products are superior to air. Figure 8 shows the effect of wall temperature variation for this case. Most of the differences here are due to the greater flux of O and NO combining exothermically to form O_2 and N_2 at the wall for the higher-wall-temperature case.

Figure 9 is for the same edge conditions as Fig. 7 but with a noncatalytic wall. The heat transfer is uniformly lower, since no recombination of air occurs in the boundary layer or at the wall. The relations have the same form as those of Fig. 3. Figure 10 shows the small effect of temperature variation for this case.

Figure 11 relates the heat transfer to the dissociation rate of ammonium chloride given by Eq. (20), as a function of the ammonium chloride interface temperature and the blunt-body radius, under the same conditions as Fig. 3 for a body of $\phi = 1.0$. The interface temperature and body radius are used to calculate the mass injection parameter, which in turn is used to determine the heat-transfer parameter. For a $\theta_{int} = 0.25$, $T_{int} = 786$ K (top two curves of Fig. 11) the heat-transfer reduction is small except for a very large blunt body radius. However, for $\theta_{int} = 0.5$, $T_{int} = 1572$ K the reduction is substantial even for very small bodies because of the much higher dissociation rate of NH_4Cl. This shows an advantage of dissociative cooling in that the cooling increases as the temperature of the body increases.

Significant heat-transfer reduction is seen to occur at even smaller radii in Fig. 12; this is the same as Fig. 11 but at the upper-atmosphere frozen-boundary-layer conditions outlined for Fig. 7, with $T_{int} = 794$ K for all cases. The reason for this greater effectiveness is that the lower ρ_e at these altitudes increases the injection parameter for a given injection rate. This is similar to the effect of body radius where κ decreases as radius increases. Figures 11 and 12 also show the NH_4Cl interface recession rate for the given interface temperature with $\phi = 1.0$ and the nose fully packed with NH_4Cl. For most cases the recession rate is very slow, and only a very small recession occurs relative to the blunt-body radius during a typical flight duration.

Conclusions

As has been shown here, transpiration cooling can provide a significant reduction in heat transfer at the stagnation point. Dissociative cooling can also provide a reduction in stagnation-point heat transfer based on the interface temperature of the dissociating

material. The effectiveness of this process increases with body radius and altitude. Another advantage of dissociative cooling is that it is self-regulating: since blowing increases with temperature, additional cooling is provided when needed most.

Appendix: Property Relations

Reasonably good estimates of property values are critical to the solution of this problem. The mixture relations[21] are particularly important. For viscosity, the relation used is

$$\mu_{\text{mix}} = \sum_i \frac{\chi_i \mu_i}{\sum_j \chi_j \Phi_{ij}} \tag{A1}$$

where $\Phi_{ij} = \sqrt{M_j/M_i}$. For thermal conductivity,

$$k_{\text{mix}} = \sum_i \frac{\chi_i k_i}{\sum_j \chi_j A_{ij}} \tag{A2}$$

$$A_{ij} = \frac{\left[1 + (k_{\text{tri}}/k_{\text{trj}})^{\frac{1}{2}} (M_i/M_j)^{\frac{1}{4}}\right]^2}{[8(1 + M_i/M_j)]^{\frac{1}{2}}} \tag{A3}$$

The binary-diffusion relation[21] between gases was taken as

$$\mathcal{D}_{ij} = \frac{0.00266 T^{\frac{3}{2}}}{P M_{ij}^{\frac{1}{2}} \sigma^2 \Omega_D} \tag{A4}$$

where $M_{ij} = 2(1/M_i + 1/M_j)^{-1}$, $\sigma_{ij} = (\sigma_i + \sigma_j)/2$, and Ω_D is a function of (kT/ε_{ij}). The multicomponent diffusion coefficients of the gas in the mixture can be approximated[22] by

$$F_{ij} = \frac{\chi_i}{\mathcal{D}_{ij}} + \frac{M_j}{M_i} \sum_{k \neq i} \frac{\chi_k}{\mathcal{D}_{ik}} \tag{A5}$$

$$D_{ij} = \frac{M}{M_j} \frac{(-1)^{i+j} A^{ij} - A^{ii}}{A} \tag{A6}$$

where A is the determinant of F_{ij}, and A^{ij} and A^{ii} are minors of A.

The results for air–helium mixtures were compared with results from Ref. 23 and were found to be reasonably close. The property relations for the injected gases and undissociated air were taken from Refs. 21, 24, and 25. For O, the collision integrals of the O–O interaction were used[26] to determine σ_O and ε_O/k as a function of temperature so that the binary-diffusion coefficients involving O could be solved for. The relations for the individual gases were compared with values[27] over a range of temperatures to ensure reasonable accuracy. Freestream air conditions as a function of altitude were obtained from Ref. 28.

Acknowledgments

This work was supported by the U.S. Army Armament Research, Development and Engineering Center (ARDEC) under Contract DAAA21-93-C-0101. The authors also wish to thank Martin Guillot for help in determining the boundary-layer edge properties.

References

[1]Reshotko, E., and Cohen, C., "Heat Transfer at the Forward Stagnation Point of Blunt Bodies," NACA TN 3513, 1955.

[2]Libby, P., "The Homogeneous Boundary Layer at an Axisymmetric Stagnation Point with Large Rates of Injection," *Journal of the Aerospace Sciences*, Vol. 29, No. 1, 1962, pp. 48–60.

[3]Hurley, D. G., "Mass Transfer Cooling in a Boundary Layer," *Aeronautical Quarterly*, Vol. 12, May 1961, pp. 165–188.

[4]Sparrow, E. M., Minkowycz, W. J., and Eckert, E. R., "The Effect of Diffusion Thermo and Thermal Diffusion for Helium Injection into Plane and Axisymmetric Stagnation Flow of Air," *Journal of Heat Transfer*, Trans. ASME, E86, Aug. 1964, pp. 311–319.

[5]Fox, H., and Libby, P., "Helium Injection into the Boundary Layer at an Axisymmetric Stagnation Point," *Journal of the Aerospace Sciences*, Vol. 29, No. 8, 1962, pp. 921–933.

[6]Sparrow, E. M., Minkowycz, W. J., and Eckert, E. R., "Diffusion-Thermo Effects in Stagnation-Point Flow of Air with Injection of Gases of Various Molecular Weights into the Boundary Layer," *AIAA Journal*, Vol. 2, No. 4, 1964, pp. 652–659.

[7]Tewfik, O. E., Eckert, E. R., and Jurewicz, L. S., "Diffusion-Thermo Effects on Heat Transfer from a Cylinder in Cross Flow," *AIAA Journal*, Vol. 1, No. 7, 1963, pp. 1537–1543.

[8]Grimaud, J. E., and McRee, L. G., "Experimental Data on Stagnation Point Gas Injection Cooling on a Hemisphere–Cone in a Hypersonic Arc Tunnel," NASA TM X-988, July 1964.

[9]Weston, K. C., "The Stagnation-Point Boundary Layer with Suction and Injection in Equilibrium Dissociating Air," NASA TN D-3889, March 1967.

[10]Henline, W. D., "Transpiration Cooling of Hypersonic Blunt Bodies with Finite Rate Surface Reactions," NASA CR 177516, Feb. 1989.

[11]Camberos, J. A., and Roberts, L., "Analysis of Internal Ablation for the Thermal Control of Aerospace Vehicles," Joint Inst. for Aeronautics and Acoustics, TR-94, Aug. 1989.

[12]Lide, D. R., *CRC Handbook of Chemistry and Physics*, 71st ed., CRC Press, 1990, p. 4-43.

[13]Anderson, J. D., *Hypersonic and High Temperature Gas Dynamics*, 1st ed., McGraw–Hill, 1989, pp. 611–634.

[14]Scala, S. M., and Gilbert, L. M., "Sublimation of Graphite at Hypersonic Speeds," *AIAA Journal*, Vol. 3, No. 9, 1965, pp. 1635–1644.

[15]Lees, L., "Laminar Heat Transfer over Blunt-Nosed Bodies at Hypersonic Flight Speeds," *Jet Propulsion*, Vol. 26, No. 4, 1956, pp. 256–269.

[16]Fay, J. A., and Riddell, F. R., "Theory of Stagnation Point Heat Transfer in Dissociated Air," *Journal of the Aeronautical Sciences*, Vol. 25, No. 2, 1958, pp. 73–85.

[17]Libby, P. A., and Pierucci, M., "Laminar Boundary Layer with Hydrogen Injection Including Multicomponent Diffusion," *AIAA Journal*, Vol. 2, No. 12, 1964, pp. 2118–2126.

[18]Howe, J. T., "Shielding of Partially Reflecting Stagnation Surfaces Against Radiation by Transpiration of an Absorbing Gas," NASA TR R-95.

[19]van Driest, E. R., "Calculation of the Stability of the Laminar Boundary Layer in a Compressible Fluid on a Flat Plate with Heat Transfer," *Journal of the Aerospace Sciences*, Vol. 19, No. 12, 1952, pp. 801–812.

[20]Virnich, H., and Höpfner, A., "Der Isotopieeffekt bei der Verdampfung von Ammoniumchlorid," *Berichte der Bunsengesellschaft für Physikalische Chemie*, Vol. 84, No. 8, 1980, pp. 716–720.

[21]Reid, R. C., Prausnitz, J. M., and Poling, B. E., *The Properties of Gases and Liquids*, 4th ed., McGraw–Hill, 1987.

[22]Cunningham, R. E., and Williams, R. J., *Diffusion in Gases and Porous Media*, 1st ed., Plenum, 1980, pp. 113–114.

[23]Eckert, E. R., Ibele, W. E., and Irvine, T. F., "Prandtl Number, Thermal Conductivity and Viscosity," NASA TN D-533, Sept. 1960.

[24]Hansen, C. F., "Approximations for the Thermodynamic and Transport Properties of High Temperature Air," NASA TR-R-50, 1959.

[25]Chase, M. W., Davies, C. A., Downey, J. R., Frurip, D. F., McDonald, R. A., and Syverud, A. N., *JANAF Thermochemical Tables*, 3rd ed., American Chemical Society and American Inst. of Physics for National Bureau of Standards, 1985.

[26]Levin, E., Partridge, H., and Stallcop, J. R., "Collision Integrals and High Temperature Transport Properties for N–N, O–O, and N–O," *Journal of Thermophysics*, Vol. 4, No. 4, 1990, pp. 469–477.

[27]Vargaftik, N. B., *Handbook of Physical Properties of Liquids and Gases, Pure Substances and Mixtures*, 2nd ed., Hemisphere, 1975.

[28]Feldman, S., *Hypersonic Gas Dynamic Charts for Equilibrium Air*, AVCO Research Lab., Jan. 1957.

I. E. Vas
Associate Editor